NKTR-214 immunotherapy synergizes with radiotherapy to stimulate systemic CD8⁺ T cell responses capable of curing multi-focal cancer

Joshua M Walker [ORCID],[1,2] Annah S Rolig,[3] Deborah H Charych,[4] Ute Hoch,[4] Melissa J Kasiewicz,[3] Daniel C Rose,[3] Michael J McNamara,[3] Ian F Hilgart-Martiszus,[3] William L Redmond [ORCID] [3]

ABSTRACT

Background High-dose radiotherapy (RT) is known to be immunogenic, but is rarely capable of driving clinically relevant abscopal antitumor immunity as monotherapy. RT is known to increase antigen presentation, type I/ II interferon responses, and immune cell trafficking to irradiated tumors. Bempegaldesleukin (NKTR-214) is a CD122-preferential interleukin 2 (IL-2) pathway agonist that has been shown to increase tumor-infiltrating lymphocytes, T cell clonality, and increase PD-1 expression. NKTR-214 has increased drug half-life, decreased toxicity, and increased CD8⁺ T cell and natural killer cell stimulation compared with IL-2.

Methods Animals bearing bilateral subcutaneous MCA-205 fibrosarcoma or CT26 colorectal tumors were treated with NKTR-214, RT, or combination therapy, and tumor growth of irradiated and abscopal lesions was assessed. Focal RT was delivered using a small animal radiation research platform. Peripheral and tumor-infiltrating immune phenotype and functional analyses were performed by flow cytometry. RNA expression profiling from both irradiated and abscopal lesions was performed using microarray.

Results We demonstrate synergy between RT of a single tumor and NKTR-214 systemic therapy resulting in dramatically increased cure rates of mice bearing bilateral tumors compared with RT or NKTR-214 therapy alone. Combination therapy resulted in increased magnitude and effector function of tumor-specific CD8⁺ T cell responses and increased trafficking of these T cells to both irradiated and distant, unirradiated, tumors.

Conclusions Given the increasing role of hypofractionated and stereotactic body RT as standard of care treatments in the management of locally advanced and metastatic cancer, these data have important implications for future clinical trial development. The combination of RT and NKTR-214 therapy potently stimulates systemic antitumor immunity and should be evaluated for the treatment of patients with locally advanced and metastatic solid tumors.

INTRODUCTION

Radiation therapy is one of the single most effective therapeutic options for many patients with solid malignancies. Used in both the curative and palliative setting, half of all patients with cancer and slightly less than one-third of all cancer survivors receive radiotherapy (RT) as part of their cancer care.[1 2] The delivery of RT has evolved significantly over the past two decades as advances in image guidance, the advent of inverse planning, and increasingly accurate dosimetry have resulted in the ability to increase dose per fraction while maintaining low levels of out of field toxicity.[3 4] Preclinical models have revealed that molecular responses to ionizing RT treatment include upregulation of major histocompatibility complex (MHC) class I,[5] increased cross-presentation of tumor antigen,[6] increased type I and II interferon expression in response to danger-associated molecular pattern signaling,[7 8] and increased expression of chemokines associated with trafficking of activated T and NK cells to the tumor microenvironment.[7 9 10] These molecular signatures of radiation, along with preclinical evidence that RT stimulates anti-tumor CD8⁺ T cell responses,[11–15] spurred great enthusiasm surrounding the prospect that RT and immunotherapy may be used in combination to synergistically stimulate tumor-specific T cell-based immunity. This enthusiasm has been bolstered by early clinical data indicating synergy between the two modalities.[16–18]

The first modern immunotherapy for cancer was recombinant interleukin 2 (IL-2), initially used to treat metastatic melanoma and renal cell carcinoma in the 1980s to 1990s.[19] Patients who experienced complete responses to high-dose (HD) IL-2 therapy frequently had durable disease control, with a subset of patients surviving disease free for greater than 20 years after being treated for metastatic disease.[19–21] However, interest in

HD IL-2 has always been limited by treatment toxicity, low response rates to therapy (objective response rates of 14%–16% and complete response rates of 5%–6%),[19 22 23] and high treatment-related mortality rates (reported as high as 2%–4% in initial studies).[19 22] As a result, administration of HD IL-2 immunotherapy has generally been limited to experienced, high-volume centers and restricted to a small subset of patients who are healthy enough to endure the potential cardiopulmonary, hepatic, renal, and neurological toxicities associated with treatment.[24]

It has been possible to reduce the toxicity of IL-2-based treatments by manipulating the half-life and the IL-2 receptor binding affinity of the drug. IL-2 signaling occurs through both dimeric IL-2Rβγ receptors present on naive, memory $CD8^+$ T, and NK cells and through trimeric IL-2Rαβγ receptors present on effector $CD8^+$ T cells and regulatory $FoxP3^+$ $CD4^+$ T cells (Treg).[25] The trimeric IL-2Rαβγ signaling complex has 10-fold to 100-fold higher affinity for IL-2 than the dimeric IL-2Rβγ, making effector $CD8^+$ T cells and $CD4^+$ Treg significantly more sensitive to the effects of IL-2 signaling than naive and memory $CD8^+$ T cell populations.[25] A primary dose-limiting toxicity of IL-2 therapy is pulmonary vascular leak. This is known to be mediated by $CD25^+$ pulmonary endothelial cells, and inhibition of IL-2Rα signaling abrogates this toxicity during IL-2 therapy.[26]

Researchers have previously used IL-2 antibody complexes and fusion proteins to bias the signaling profile in favor of the IL-2Rβ chain (CD122) and decrease affinity for IL-2Rα chain, and there is evidence that CD122 biased IL-2 complexes synergize more effectively with immunogenic RT regimens than uncomplexed IL-2.[26–28] These modifications also greatly enhance the half-life of recombinant IL-2 in vivo, extending the half-life of recombinant IL-2 by an order of magnitude or more.[26 27 29 30] One successful modification of IL-2 has been NKTR-214, a polyethylene glycol (PEG)-bound prodrug formulation of recombinant IL-2.[31 32] This drug has, on average, six releasable PEG chains that extend the half-life and alter the binding affinity of the recombinant IL-2 in vivo, biasing binding in favor of CD122 over CD25 and resulting in increased Teff/Treg ratios in tumor tissue from mice treated with NKTR-214 versus native IL-2.[31 32] In animal models, NKTR-214 also exhibits more robust antitumor activity as a monotherapy than recombinant IL-2, synergizes with CTLA-4 blockade to result in significantly increased tumor clearance compared with either drug alone, and does not result in hypotension or vascular leak syndrome.[32] NKTR-214 is now in clinical trials in combination with PD-1 blockade, with promising early results.[33–35]

There is now early clinical data demonstrating synergy between HD IL-2 and stereotactic RT,[17] preclinical data indicating NKTR-214 stimulates robust antitumor immunity with limited toxicity,[32] and evidence that RT stimulates antitumor immunity by upregulating antigen presentation and T cell trafficking to the tumor microenvironment.[6 7 9 10] We investigated the potential synergy and underlying mechanisms of action between HD single fraction RT and NKTR-214 therapy. Our results reveal that the combination of RT plus NKTR-214 significantly improves control of irradiated and distant (unirradiated) tumor growth, markedly increases survival of animals bearing multiple tumors, increases $CD8^+$ T cell trafficking to all disease sites, and increases effector function of tumor-infiltrating $CD8^+$ T cells. Together, these data provide insight into the mechanisms through which NKTR-214/RT synergize to elicit potent systemic antitumor immunity and support the clinical evaluation of NKTR-214/RT immunotherapy.

MATERIALS AND METHODS
Mice
Wild-type 6–8-week-old C57BL/6 and BALB/c mice were purchased from Jackson Labs (Bar Harbor, Maine, USA). Mice bearing the Nur77-GFP transgene were kindly provided by Dr Andrew Weinberg (Earle A. Chiles Research Institute, Portland, Oregon, USA).[36] All mice were maintained under specific pathogen-free conditions in the Providence Portland Medical Center animal facility. Experimental procedures were performed according to the National Institutes of Health Guide for the Care and Use of Laboratory Animals and in accordance with the Earle A. Chiles Research Institute Institutional Animal Care and Use Committee (Animal Welfare Assurance No. A3913–01).

Tumor models and treatment regimens
This study used CT26 (colon carcinoma, BALB/c, female, subcutaneous, $1×10^6$) and MCA-205 (fibrosarcoma, C57BL/6, female, subcutaneous, $1×10^6$) tumor cell lines. The CT26 tumor line was obtained from American Type Culture Collection (ATCC) and MCA-205 was generously provided by Dr Andrew Weinberg (Earle A. Chiles Research Institute). Tumor lines are tested annually using the MycoAlert mycoplasma detection kit (Lonza, Basel, Switzerland). Treatments began 10 days following implant. Mice in this study received either control (diluent; 10 mM citric acid, 7% trehalose, pH 4), radiation therapy, NKTR-214 (Nektar, San Francisco, California, USA, 0.8 mg/kg, intravenous),[32] rhIL-2 (88 500 IU injection, three times per day), RT/NKTR-214, or RT/rhIL-2. CT-guided photon RT with a beam energy of 220 kV was delivered using a small animal radiation research platform (XStrahl, Gulmay Medical, Suwanee, Georgia, USA) to an isocenter in the center of the tumor. Dosimetry was performed using Murislice software (XStrahl) and irradiated lesions received 16 Gy in a single fraction using opposed tangential fields. Tumor growth was monitored using two-dimensional (length × width) caliper measurements three times per week until all animals in the cohort reached a primary endpoint (tumor free or tumor burden >250 mm^2), or for tumor harvest experiments, tumors were harvested 7 days post-treatment. In

NK, CD4, and CD8 depletion experiments animals were treated using 20 µL anti-asialo-GM1 (Biolegend, resuspended in 1 mL sterile water) delivered once intraperitoneally 1 day before treatment, 200 µg anti-CD4 (clone GK1.5) given one time per week intraperitoneally for 6 weeks, or 200 µg anti-CD8 (clone 53-6.7) delivered once intraperitoneally on day 9, 1 day before treatment. For statistical analyses, endpoints were defined as the first time point that tumor area exceeded 250 mm^2 or was non-palpable and did not subsequently recur at the site.

Blood and tumor collection and processing

Blood samples were drawn from CT26 tumor-bearing mice on day 7 post-treatment. For each sample, 25 µL of fresh heparinized blood was incubated with the appropriate dilution of fluorescence-conjugated antibodies (see Flow cytometry section) for 30 min at 4°C in the dark. Tumors were harvested 7 days post-treatment, cut into small fragments, and digested in 1 mg/mL collagenase and 20 mg/mL deoxyribonuclease (DNase) (Sigma) in phosphate buffered saline for 45 min at room temperature. Subsequently, tumor-infiltrating lymphocytes (TILs) were filtered through 70 µm nylon mesh (Cell Treat), washed with 10 mL complete Roswell Park Memorial Institute media (RPMI), and collected by centrifugation (1500 rpm, 4 min). Pelleted cells were resuspended for staining and analysis by flow cytometry (see Flow cytometry section).

Flow cytometry

For blood and tumor lymphocyte phenotyping, blood or tumor was stained for 30 min in the dark with the following surface markers: CD4, CD8, NKp46, ICOS, PD-1, Tim-3, CD122, and/or AH1-A5 tetramer. Next, cells were fixed and permeabilized following manufacturer's instructions (FoxP3/Transcription Factor Staining Buffer Set, ThermoFisher, San Diego, California, USA) and stained for the following intracellular targets: Granzyme A, FoxP3, and/or Ki-67. To examine IFN-γ and TNF-α expression, prior to staining, cells were incubated in a 96-well round bottom plate coated with agonistic aCD3/aCD28 (100 µL solution per well of aCD3 (145–2 C11, BD Biosciences, San Jose, California, USA) and aCD28 (37.5.1, BD Biosciences) at 5 µg/mL and 2 µg/mL concentrations, respectively). Plates were incubated for 4 hours in standard cell culture conditions (37°C, 5% CO_2, 95% humidity). Following incubation, cells were washed and stained as described above. Flow cytometry data were acquired on an LSR II flow cytometer running FACSDiva software (BD Biosciences) and data were processed and analyzed with FlowJo (Treestar, Ashland, Oregon, USA). All antibodies for flow cytometry were obtained from ThermoFisher (San Diego, California, USA) or BD Biosciences.

RNA isolation and processing

Eight days post-treatment, tumors from CT26 bearing mice (n=3/group) were harvested for RNA isolation and processing. Total RNA from the tumors was harvested using an RNeasy kit (Qiagen, Hilden, Germany) according to the manufacturer's instructions. The RNA samples were then sent to the Oregon Health and Science University Gene Microarray Shared Resource (Beaverton, Oregon, USA) for analysis. The core facility produced cRNA from the samples and then probed the Affymetrix 430 2.0 array. Analysis was performed using Affymetrix software. Heatmaps and statistical analysis were performed using R. CIBERSORT was used to infer leukocyte representation from the bulk RNA.[37]

Statistical analysis

Throughout the manuscript, data are presented in box and whisker plots, which display the data median (line within the box), the box spans the IQR, and the whiskers extend to the highest and lowest observations. One-way analysis of variance (ANOVA) was used to compare overall differences among the groups and Dunnett's multiple comparison test was used to compare each group against the combination treatment. Spearman's correlation was used to correlate blood and tumor immune populations with tumor size and Kaplan-Meier plot and log-rank tests were used for tumor survival analysis. All statistical analysis were performed using GraphPad Prism software (GraphPad, San Diego, California, USA) or R. A p value of <0.05 was considered significant.

RESULTS

NKTR-214 and RT synergize to control abscopal tumor growth and promote survival

In order to test the hypothesis that combination treatment with NKTR-214 and RT would improve disease control and abscopal responses, we utilized two bilateral flank tumor models. CT26 (colon carcinoma) or MCA-205 (fibrosarcoma) tumors were established subcutaneously in the bilateral flanks of wild-type BALB/c or C57BL/6 mice, respectively. Ten days following implantation, once the cumulative tumor burden had reached approximately 50–100 mm^2, animals received 16 Gy RT alone to a single flank tumor (RT), intravenous NKTR-214 therapy (0.8 mg/kg; NKTR-214), or combination therapy (NKTR-214/RT). We selected the RT dose because it provided temporary control, but not cure, in 70%–90% of lesions treated with monotherapy and had no effect on out of field lesions on the opposite flank. Subsequently, tumor growth was assessed, and in additional cohorts, effects on TIL phenotype and function were investigated 7 days post-treatment (day 17 postimplant, figure 1A). We observed a significant improvement in overall survival in both tumor models when animals received combination therapy as compared with controls or animals receiving monotherapy with either RT or NKTR-214 (figure 1B). Although RT alone caused growth delay, and in some cases cured the irradiated tumor, it did not result in a systemic abscopal response capable of controlling contralateral unirradiated tumor (figure 1C). In contrast, NKTR-214 monotherapy cured bilateral disease in 25%–29%
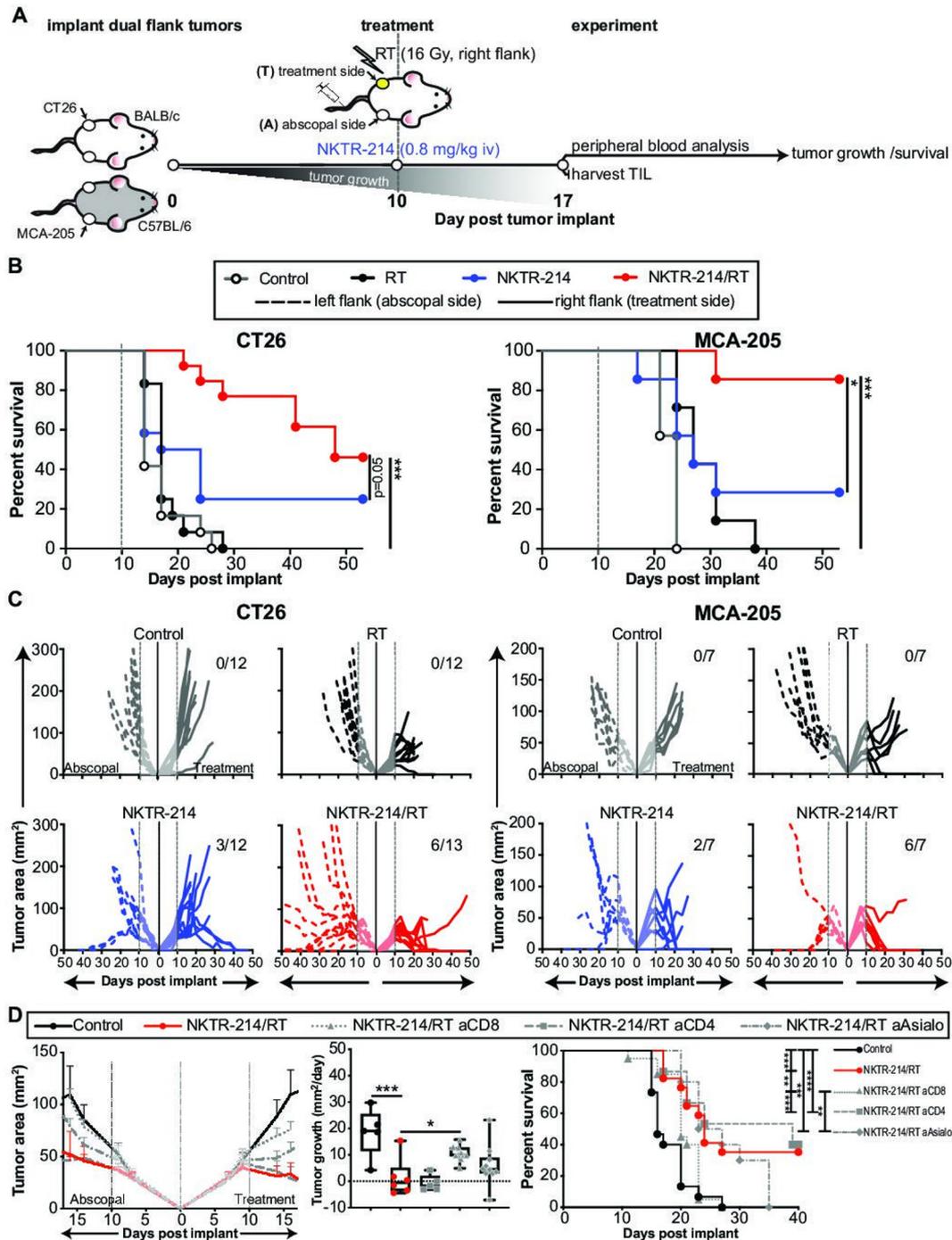
Figure 1 NKTR-214/RT combination treatment decreases tumor growth and increases survival. (A) Schematic of experimental protocol. (B, C) Wild-type BALB/c (left panels) or C57BL/6 (right panels) received either CT26 (n=12/group) or MCA-205 (n=7/group) tumor cells, respectively. Tumor-bearing mice were treated with RT (16 Gy, right flank) and/or NKTR-214 (0.8 mg/kg, intravenous) 10 days post tumor implant, survival (B) and tumor growth (C) were assessed. in panel (C) dotted lines represent tumor growth on the abscopal side, solid lines represent tumor growth on the treatment side. Numbers in the upper right corner of graphs indicate the number of mice with complete cures. (D) CT26 tumor-bearing animals were CD4, CD8, or NK-depleted on day 9 followed by treatment with vehicle control or combination RT/NKTR-214 on day 10, and animals were subsequently assessed for tumor growth and survival. Depletion graphs represent n=10–19 animals/group over 1 (for NK cell depletion) or 2 (for CD8^{+} and CD4^{+} T cell depletions) independent experiments. Treatment with NKTR-214/RT significantly reduced tumor growth (mm²/day) and increased survival in comparison to vehicle control, an effect that was lost in the absence of CD8^{+} T cells. Statistics show a one-way ANOVA Dunnett's test comparing each group to NKTR-214/RT combination or a log-rank test for Kaplan-Meier survival plots. ANOVA and log-rank significance: *P<0.05, **P<0.01, ***P<0.001, ****P<0.0001. ANOVA, analysis of variance; RT, radiotherapy.

of animals. Remarkably, combination NKTR-214/RT therapy significantly increased response rates leading to cures in 58%–86% of animals, depending on the model (figure 1C). We note that this was a significantly greater tumor control and overall survival than that achieved by combination therapy with recombinant human (rhIL-2)/RT (online supplementary figure 1A).

To determine the role of NK, CD4^{+}, and CD8^{+} T cell compartments in the response to therapy, animals underwent NK, CD4^{+}, or CD8^{+} T cell depletion after tumors had been established and prior to treatment with combination NKTR-214/RT. Animals undergoing CD4^{+} T cell depletion experienced the same reduction in tumor growth observed in the combination treatment, while CD8^{+} T cell depletion completely abrogated therapeutic efficacy. CD8^{+} T cell depletion of NKTR-214/RT treated animals resulted in both increased tumor growth (mm²/day) and decreased survival compared with the CD8^{+} T cell replete NKTR-214/RT cohort (figure 1D). Animals that underwent NK depletion had an intermediate phenotype, evidenced by significantly improved tumor control and survival compared with untreated controls (p<0.001) or CD8-depleted animals (p<0.01). However, NK-depleted animals had slightly decreased tumor control compared with CD4-depleted or immunologically intact animals, though this was not statistically significant. This data suggest that CD8^{+} T cells are the primary driver of the antitumor response to combination therapy (figure 1D).

Combined NKTR-214/RT therapy increases the relative percentage of peripheral CD8^{+} T cells, which correlates with tumor control

Because we observed a striking reduction in abscopal tumor size following NKTR-214/RT treatment, we asked how combined treatment influenced systemic immune responses by immunophenotyping peripheral blood. For the following experiments, we focused on the CT26 model, which allowed us to track tumor-specific (AH1 tetramer[+]) responses.[38] Tumors were established in mice, and the mice received therapy as described previously (figure 1A). One week following treatment, peripheral blood immunophenotyping was performed and percentages of CD8^{+}, FoxP3^{−} CD4^{+} T effector (Teff) cells, FoxP3^{+} CD4^{+} T regulatory (Treg) cells, and NKp46^{+} NK cells were determined (figure 2A). Combination therapy resulted in statistically significant increases in the percentage of circulating lymphocytes comprised of CD8^{+} T cells compared with vehicle controls or monotherapies with RT or NKTR-214 alone (figure 2B). Circulating levels of NK cells were elevated in all animals receiving NKTR-214, whether alone or in combination with RT. While there was no effect on the overall percentage of circulating CD4^{+} T cells, treatment with NKTR-214 alone resulted in an increase in Treg within the CD4^{+} T cell compartment compared with RT or vehicle control. However, NKTR-214/RT combination therapy significantly decreased the fraction of Treg
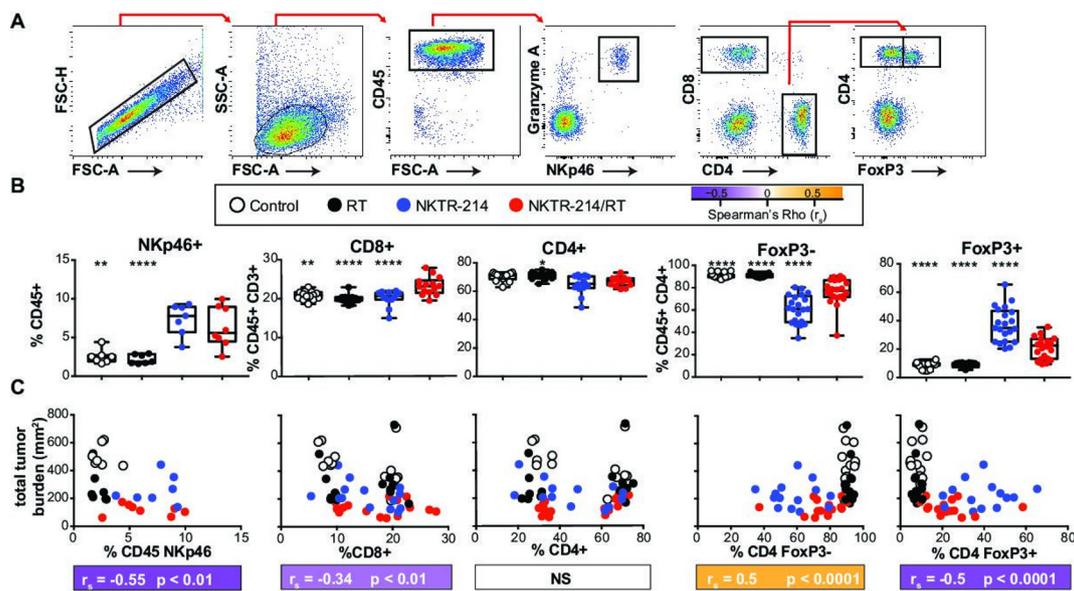

Figure 2 NKTR-214/RT combination treatment induces systemic CD8^{+} T cell responses that correlate with a reduction in total tumor burden. CT26 tumors were implanted into bilateral flanks on day 0. Established tumors were treated (NKTR-214 +/− RT) day 10 postimplant and blood was drawn 17 days postimplant to investigate systemic effects of treatment. (A) Representative dot plots of gating strategy are depicted. (B) NKTR-214/RT combination treatment (red circles) induces a significantly greater per cent of CD8^{+} T cells than the vehicle control (open circles), RT alone (black circles), or NKTR-214 alone (blue circles). Data shown from either one (NKp46^{+}; n=7), two (CD4^{+}, CD8^{+}; n=14), or three (FoxP3^{−}, Foxp3^{+}; n=21) independent experiments. Statistics show a one-way ANOVA Dunnett's test comparing each group to NKTR-214/RT combination. (C) Correlation between each cell type and the total tumor burden (treatment and abscopal side) measured on day 17. Colored bar below graph depicts strength of Spearman's correlation (r_s) and the statistical significance of that correlation. All plots show data from two independent experiments (n=14), except NKp46, which shows one experiment (n=7). *P<0.05, **P<0.01, ***P<0.001, ****P<0.0001. ANOVA, analysis of variance; RT, radiotherapy; FSC, forward scatter; SSC, side scatter.

CD4$^+$ T cells compared with NKTR-214 monotherapy (figure 2B). NKTR-214/RT therapy also resulted in an increased frequency of CD8$^+$ T cells, Tregs, and NK cells compared with combination therapy with rhIL-2/RT (online supplementary figure 1B). These results suggest that combined RT/NKTR-214 treatment alters the adaptive immune response by increasing the frequency of circulating cytotoxic CD8$^+$ T cells while decreasing Treg percentages compared with monotherapy.

To determine if these changes in systemic adaptive immune responses were associated with changes in tumor burden, the levels of each peripheral blood cell type were compared with total tumor area using Spearman's correlations (figure 2C). These data revealed significant negative associations between levels of circulating CD8$^+$ T, NK, and Treg cells and reduced total tumor burden. Interestingly, while the relationship between CD8$^+$ T and NK cells appears to be linear across treatment groups (simple linear regression: CD8$^+$ r^2=0.08, p<0.05; NK r^2=0.2, p<0.05, regression lines not shown), the relationship between Tregs and tumor burden appears to be driven entirely by NKTR-214-driven changes to peripheral CD4$^+$ phenotypes. In fact, if analysis is carried out only on mice receiving NKTR-214, then the negative association between Tregs and tumor burden actually becomes a non-statistically significant positive association (online supplementary figure 2, simple linear regression: r^2=0.07, p=0.14). This positive correlation suggests that in NKTR-214-treated animals, higher numbers of Tregs are more likely to be found in larger tumors. The linear relationship observed between CD8$^+$ T cells agrees with our CD8$^+$ T cell depletion experiments (figure 1D) and highlights the impact of CD8$^+$ T cells on the reduction of tumor burden in combination-treated animals.

NKTR-214/RT does not significantly increase peripheral CD8$^+$ T cell activation compared to NKTR-214 monotherapy

In addition to the changes observed in the relative proportions of cell types in the peripheral immune response (figure 2B), we also assessed whether the phenotype and activation state of these cells were altered. Based on the correlation between increased CD8$^+$ T cells and reduced tumor burden, we hypothesized that combination treatment with NKTR-214/RT would result in increased levels of activation and proliferation within CD8$^+$ T cell populations. However, we found that NKTR-214 monotherapy increased levels of several activation markers on CD8$^+$ T cells, but these effects were not enhanced by the addition of RT. Specifically, we observed that NKTR-214 monotherapy increased CD8$^+$ T cell expression of the activation and exhaustion marker PD-1, activation and proliferation markers CD122 (IL-2Rβ) and Ki-67, and increased expression of the effector molecule granzyme A compared with controls (figure 3A,B). The addition of concurrent RT did not significantly increase any of these proteins in peripheral CD8$^+$ T cells over NKTR-214 monotherapy.

While PD-1 and Tim-3 are known to be upregulated on functionally exhausted CD8$^+$ T cells,[39 40] these antigens are also upregulated during acute T cell activation.[38] Inducible T cell co-stimulator (ICOS) is a CD28 family costimulatory molecule known to be absent on naive CD4$^+$ and CD8$^+$ T cells but is rapidly induced in subsets of T cells following activation.[41 42] We found the percentage of ICOS and Tim-3 expressing CD8$^+$ T cells was significantly increased in animals receiving combination therapy compared with control groups (figure 3B), consistent with recent activation. Therapy with NKTR-214/RT also increased significantly the percentage of circulating CD8$^+$ T cells expressing the activation/effector molecules PD-1, Ki-67, granzyme A, and CD122 compared with combined rhIL-2/RT therapy (online supplementary figure 1B). Thus, we found increased CD8$^+$ T cell activation and proliferation in animals receiving NKTR-214 therapy (figure 3B) and evidence of increased relative percentage of these cells in the periphery (figure 2) in animals undergoing NKTR-214/RT. Further, these markers of activation (PD-1, Ki-67, CD122, Tim-3, and GzmA) correlated with decreased tumor area measurements using Spearman's correlations (figure 3B).

Unlike the CD8$^+$ T cells, expression of these surface markers on peripheral CD4$^+$ Teff or Treg populations did not show strong correlations with tumor burden. In CD4$^+$ Teff cells treated with NKTR-214 monotherapy, we observed significant increases in the percentage of cells expressing the activation/proliferation markers CD122 and Ki-67, but no further increase in frequency when concurrent RT was added to NKTR-214 treatment (figure 3C). However, analysis of Treg cell populations revealed a very different pattern of expression. We observed significant increases in percentages of PD-1 and ICOS-expressing Treg cells in the blood of animals receiving NKTR-214 monotherapy, but these increases were lost when animals were treated concurrently with RT. Additionally, animals receiving either NKTR-214 monotherapy or NKTR-214/RT combination therapy had a lower frequency of peripheral Ki-67$^+$ Treg cells than animals receiving vehicle control or RT alone (figure 3D). Together, these results indicate that NKTR-214 monotherapy increases Teff cell proliferation and decreases Treg cell proliferation in the circulation over RT and vehicle controls. Furthermore, systemic Treg cell activation (ICOS/CD122) secondary to NKTR-214 monotherapy can be tempered by adding local RT.

NKTR-214/RT combination therapy results in increased T cell expansion, proliferation, and function within irradiated and abscopal disease sites, correlating with increased tumor control

Given the remarkable control of contralateral tumors (figure 1) and systemic increase in CD8$^+$ T cells (figure 2), we asked whether the immune responses present in the treated and abscopal tumor sites reflected what was observed in the peripheral blood and whether this was correlated with tumor control. CT26 tumors were established as described above (figure 1) and tumors were harvested 7 days following treatment. In order to account for variable tumor sizes between animals, results are
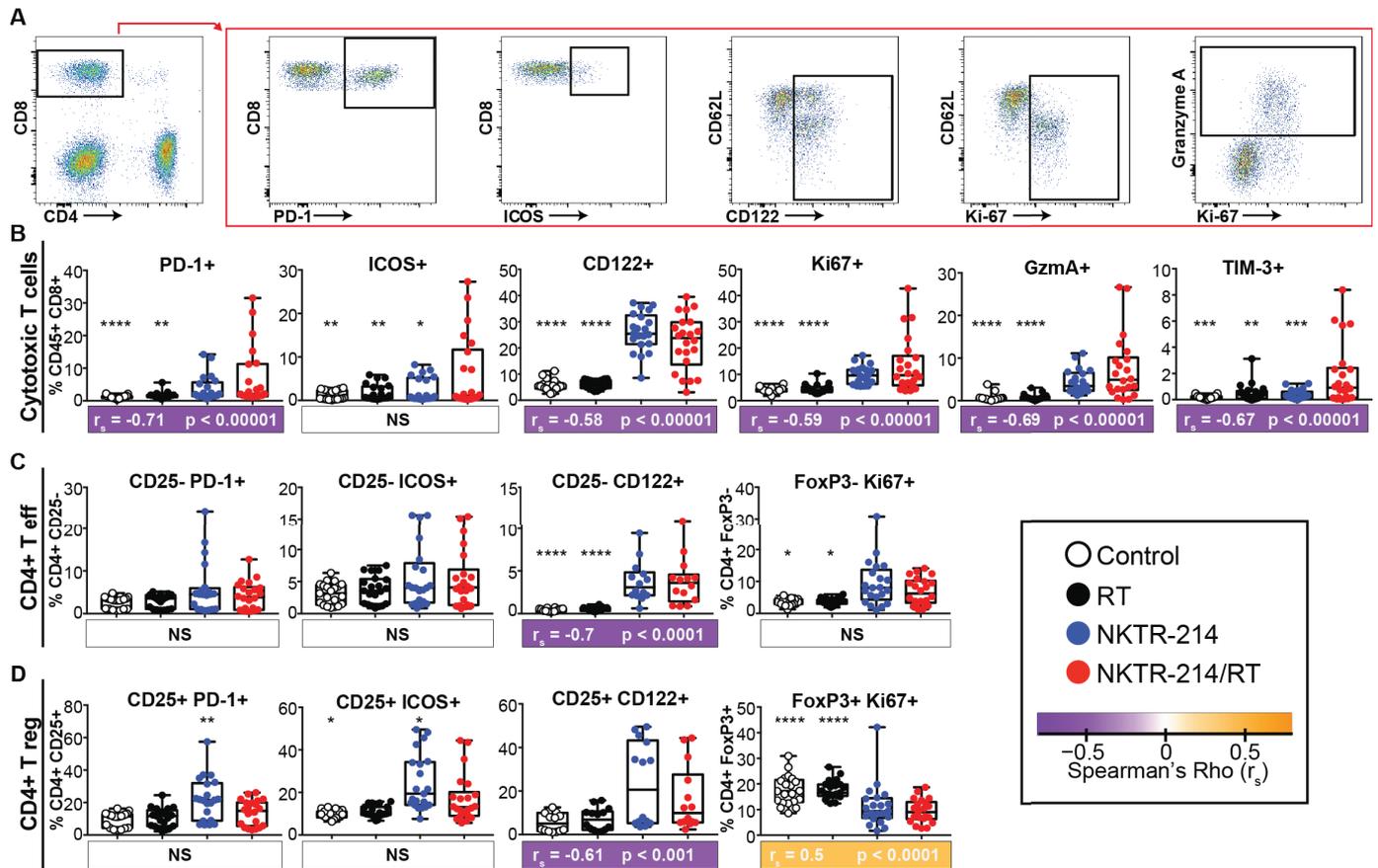
Figure 3 NKTR-214/RT combination treatment induces markers of CD8$^+$ T cell activity that correlate with a reduction in total tumor burden. CT26 tumors were implanted into bilateral flanks, animals treated, and peripheral blood harvested as previously described in figure 2. Representative dot plots of CD8$^+$ T cell exhaustion, activation, and proliferation markers are demonstrated (A). Differences in markers identifying subsets of CD8$^+$ T cells (B), Teff cells (CD25$^-$ or FoxP3$^-$) (C), and Treg cells (CD25$^+$ or Foxp3$^+$) (D) following monotherapy and NKTR-214/RT combination treatment. Data shown from either two or three independent experiments (n=14–21). Statistics show a one-way ANOVA Dunnett's test comparing each group to NKTR-214/RT combination group. *P<0.05, **P<0.01, ***P<0.001, ****P<0.0001. Spearman's correlations of each cell subset with total tumor burden measured on day 17 are represented as a colored box below each graph. The color represents r$_s$, statistics indicated by p value. All correlations are from the combined data of two independent experiments (n=14). ANOVA, analysis of variance; RT, radiotherapy; Teff, T effector; Treg, T regulatory.

reported as absolute number of cells per mm^2 of tumor (figure 4) as well as percentage of overall leukocytes (online supplementary figure 3). We found that dual therapy resulted in significantly increased CD8$^+$ T cell density within both the irradiated and abscopal lesions compared with all control groups (figure 4A). Similarly, an increased density of Ki-67$^+$, ICOS$^+$, PD-1$^+$, and Tim-3$^+$ CD8$^+$ T cells was observed following dual therapy in the irradiated and abscopal tumors (figure 4A). We further characterized the TILs by determining the density and frequency of tumor-specific AH1$^+$ CD8$^+$ T cells using peptide–MHC tetramers.[38] We discovered that NKTR-214/RT combination therapy resulted in a non-significant increase in density of AH1$^+$ CD8$^+$ T cells within irradiated tumors and a significant increase in AH1$^+$ CD8$^+$ T cell density within abscopal tumors compared with NKTR-214 monotherapy (figure 4A).

We also assessed the extent of T cell-specific cytokine production following anti-CD3/anti-CD28 re-stimulation in vitro. We observed increased effector function of tumor-specific CD8$^+$ T cells in animals treated with NKTR-214/RT compared with controls within the irradiated and abscopal lesions, as evidenced by an increased density of TIL from combination treated animals expressing IFN-γ, TNF-α, and granzyme A. Notably, NKTR-214/RT therapy also increased the frequency of CD8$^+$ T cells expressing IFN-γ and TNF-α (online supplementary figure 3). Finally, the increase in density of these CD8$^+$ T cell phenotypes correlated with tumor burden both on the treatment side and on the abscopal side (figure 4A). However, this increased activity did not appear to be due to increased T cell receptor ligation. To address this, we utilized the transgenic Nur77 fluorescent reporter mouse in which the strength of T cell receptor stimulation correlates directly with GFP expression.[36] We did not observe a significant increase in T cell receptor signaling following combination treatment (online supplementary figure 4). While we saw an increased NK cell frequency in the peripheral blood following treatment with NKTR-214 (figure 2B), which strongly associated with tumor burden, we did not
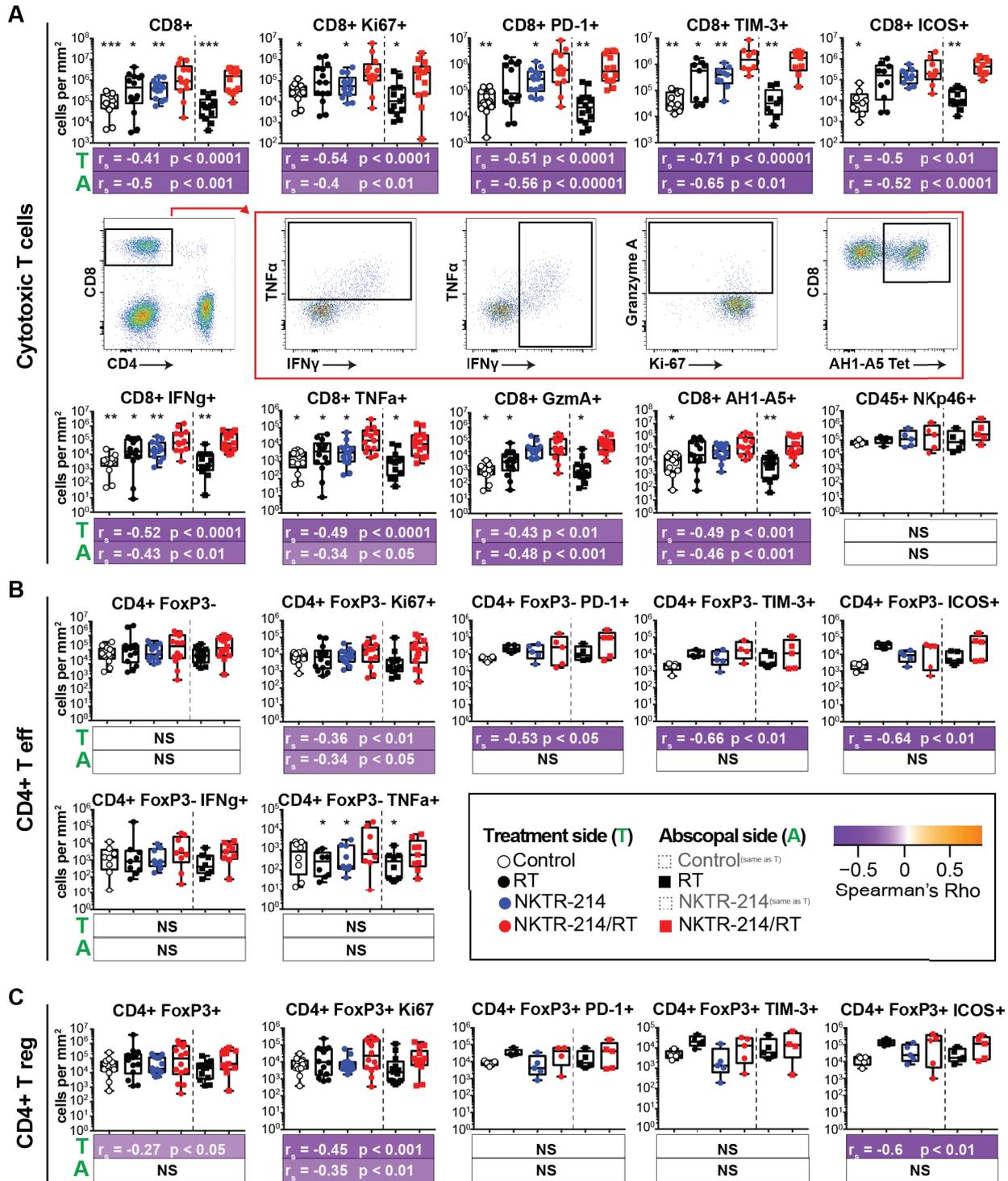
Figure 4 NKTR-214/RT combination treatment induces increased CD8+ T cell intratumoral density that correlates with reduction in tumor size. CT26 tumors were implanted into bilateral flanks on day 0. Established tumors were treated (NKTR-214 +/– RT) day 10 postimplant and tumors were harvested 17 days postimplant. CD8+ T cell (A), CD4+ Teff (FoxP3−) (B), or Treg cell (Foxp3+) (C) phenotype densities in treatment side (circles) and abscopal side (squares) tumors. Tumor-specific CD8+ T cells were identified using AH1-A5 specific peptide–MHC tetramers. Data shown from two independent experiments (n=14). Spearman's correlations of each cell subset from either treatment side (T) or abscopal side (A) with the corresponding tumor size on harvest day. For all box and whisker plots, statistics show a one-way ANOVA Dunnett's test comparing each group to the NKTR-214/RT combination group within the same treatment side. *P<0.05, **P<0.01, ***P<0.001, ****P<0.0001. For Spearman's correlations color represents r_s, statistics are indicated by p value. ANOVA, analysis of variance; RT, radiotherapy; Teff, T effector; Treg, T regulatory.

observe an increase in density (figure 4A) or frequency (online supplementary figure 3) of NK cells in the TIL.

As we observed in the peripheral blood, the differences between treatment groups when assessing the density, frequency, and function of CD4+ T cells within the TIL were not striking. Numbers of CD4+ Teff cells were unchanged among the groups, with no effect observed following monotherapy or combination therapy with NKTR-214 or RT in any group (figure 4B). Similarly, there were no observed differences among treatment groups when measuring numbers of Teff cells expressing activation, exhaustion, or proliferation markers (figure 4B). There was some evidence of increased effector function in Teff cell following aCD3/aCD28 stimulation, with slightly increased numbers of TNF-α-expressing cells in irradiated and abscopal lesions following combination therapy. In the Treg cell population, we did not observe any differences in the frequency, activation state, proliferation, or function in any treatment group compared with controls (figure 4C). Across groups, with the exception of Teff and Treg Ki-67, no CD4+ T cell marker exhibited a correlation with abscopal side tumor burden, further supporting our depletion data and suggesting no major role for CD4+ T cells in combination therapy with NKTR-214/RT.

RNA expression analysis reveals increased effector function and upregulation of T cell trafficking-related transcripts within treated and abscopal lesions following NKTR-214/RT therapy

Following our observation that NKTR-214/RT therapy resulted in increased CD8+ T cell frequency, activation, and effector function within the tumor microenvironment of the irradiated lesion and the non-irradiated lesion, we asked what mediated the increased abscopal response. Thus, we isolated mRNA from bilateral whole tumor lysates in all treatment groups, 8 days following treatment and performed gene expression analysis. These data were initially analyzed using CIBERSORT[37] deconvolution algorithm which provided evidence consistent with our TIL analysis of increased T cell infiltration within tumors in animals treated with RT or NKTR-214 monotherapy or NKTR-214/RT compared with controls. Notably for the combination treatment, increases in T cell infiltration were observed in irradiated as well as abscopal lesions (figure 5A). In order to gain insight into possible mechanisms of the potent antitumor effects observed in irradiated and abscopal lesions in animals receiving combination NKTR-214/RT, we analyzed the RNA expression data based on functional groups focused on cytotoxic effector function (figure 5B), tissue leukocyte recruitment (figure 5C), and lymphocyte expression of homing markers (figure 5D). For each gene in these categories, the change in gene expression compared with vehicle control are shown for RT, NKTR-214, or the NKTR-214/RT combination group. As expected, the data revealed dramatic NKTR-214-driven increases in effector molecule expression, such as granzymes, perforin, and TNFα within the tumors of all animals receiving

NKTR-214 (figure 5B and C). The addition of RT to NKTR-214 did not significantly increase these responses over NKTR-214 monotherapy on either the treated or abscopal side (figure 5B).

We observed some increased expression of T cell chemoattractant chemokines, such as CCL4, CCL5, and CXCL10 on the abscopal side in animals receiving NKTR-214/RT combination therapy compared with NKTR-214 alone or RT alone (figure 5C). These chemokines are known to be induced intratumorally in response to RT[7 43]; however, here we demonstrate the combination of NKTR-214/RT induces expression of these chemokines associated with T cell recruitment in the abscopal lesion as well. There were also several genes associated with lymphocyte homing that were increased in the abscopal treatment site following combination therapy in comparison to NKTR-214 alone. These genes appear to fit into two broad categories, macrophage recruitment and function (CMKLR1, CSF1R, CX3CR1) and lymphocyte migration and adhesion (CCR5, ITGA9, CCRL2, figure 5D). Interestingly, when we used flow cytometry to assess CSF1R and CX3CR1 expression within the tumor microenvironment following treatment with NKTR-214 monotherapy or NKTR-214/RT combination therapy, we observed significantly decreased expression of these molecules within dendritic cell, tumor-associated macrophage, and myeloid-derived suppressor cell populations, but significantly increased expression within the CD45− population (online supplementary figure 5). These results indicate changes in expression of these homing molecules may be driven by treatment effects on the tumor itself or other elements within the tumor stroma not evaluated in these assays. Taken together with our flow cytometry-based TIL phenotyping, these data suggest that the combination of NKTR-214/RT may result in increased expression of a variety of genes at the treated and abscopal sites that promote lymphocyte recruitment and retention in the tumors, which ultimately is associated with significantly improved survival.

DISCUSSION

RT remains one of the single most effective therapies in the definitive and palliative treatment of solid tumors, and immunomodulation has emerged over the past two decades as one of the most promising therapies for patients with locally advanced and metastatic disease. During the time immunotherapy has become the standard of care to treat metastatic disease in a wide variety of tumor types, RT has benefited from technical advances such that cranial radiosurgery and extracranial ablative RT that are now part of the routine practice of radiation medicine in both academic and community practice settings. Starting with HD IL-2 as the first modern immunotherapy, the practice of immunomodulation has revolutionized the treatment of locally advanced and metastatic cancer over the past 30 years and now includes immune checkpoint inhibitors that block CTLA-4 and PD-1. Initial
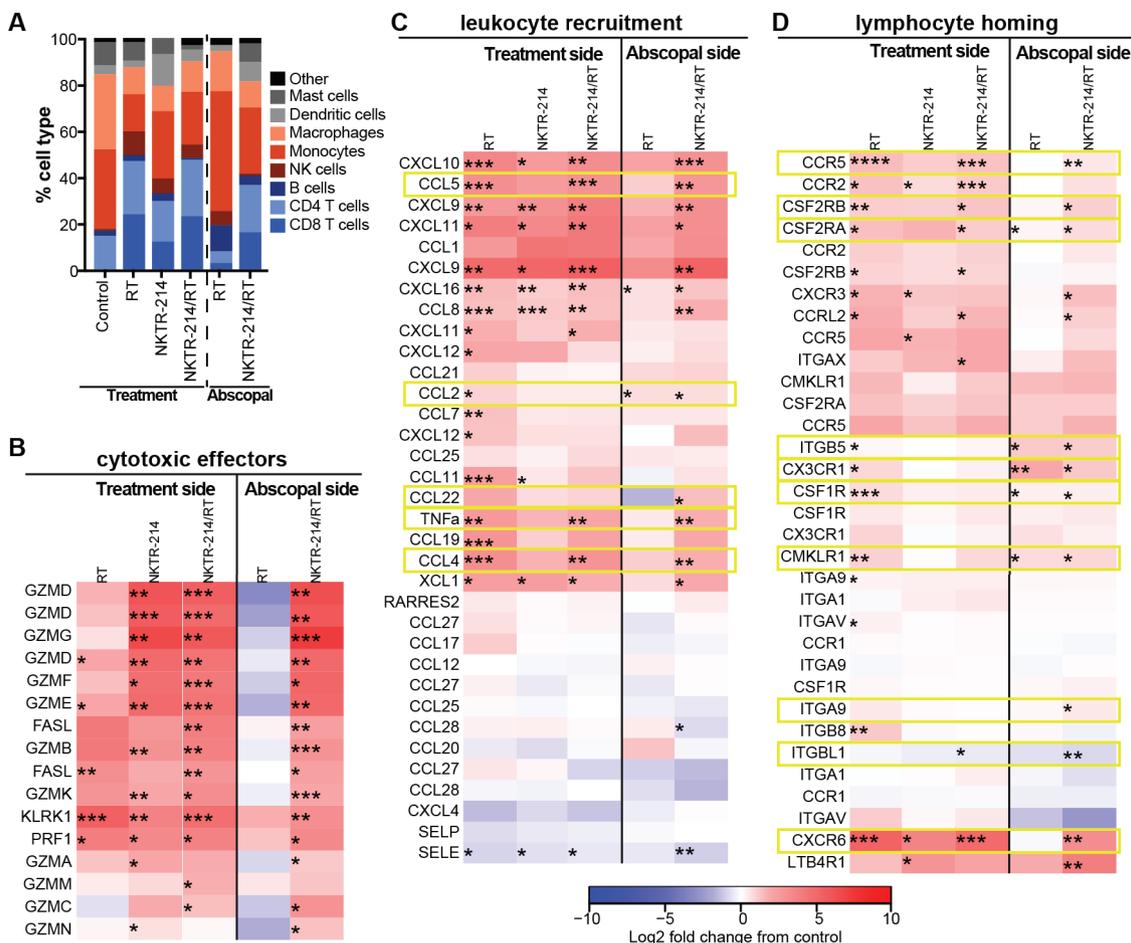
Figure 5 RT increases lymphocyte homing genes on the treatment and abscopal sides. Eight days post-treatment, tumors from CT26-bearing mice were processed for RNA isolation for gene expression analysis with Mouse Affymetrix 430 2.0 arrays (n=3 biological replicates per group). Not false discovery rate corrected prior to statistical analysis. (A) CIBERSORT analysis of the RNA indicates an expanded proportion of CD8^{+} T cells in the treatment and abscopal tumors from mice that received NKTR-214/RT combination treatment. (B, C, D) Change in gene expression compared with vehicle control are shown for RT, NKTR-214, or the NKTR-214/RT combination group. vehicle control is the reference for all log fold-changes and thus is not shown separately. RT enhances expression of leukocyte recruitment and lymphocyte homing genes both alone and in combination with NKTR-214. RT and NKTR-214 alone can induce genes related to lymphocyte homing on the treatment side, but only RT can induce those genes on the abscopal side. NKTR-214 alone induces systemic cytotoxic effector genes. Thus, combination of NKTR-214/RT increases homing and recruitment of active CD8^{+} T cells that reduce tumor burden. *P<0.05, **P<0.01, ***P<0.001, ****P<0.0001. RT, radiotherapy.

clinical trials with CTLA-4 and PD-1 blockade in patients with metastatic melanoma demonstrated dramatic increases in progression-free survival and overall survival compared with conventional therapy and patients experienced significantly less toxicity than those receiving HD IL-2 therapy.[44–48] This response has now been seen in a number of other disease sites, including renal cell carcinoma,[49] non-small cell lung cancer,[50–52] hepatocellular carcinoma,[53] and head and neck squamous cell carcinoma.[54]

Following a number of case reports and preclinical studies combining RT and immunotherapy, there has been great enthusiasm for treatments utilizing both modalities. These clinical data are supported by evidence that RT is capable of upregulating antigen presentation,[6] driving type I and II interferon responses,[7 8] and driving T and NK cell trafficking to the tumor microenvironment.[7 9 10]

Here we report preclinical results from the combination of NKTR-214, a CD122-biased PEGylated recombinant IL-2, with radiation therapy. We found significant synergy between these modalities; combination treatment with NKTR-214 and RT promotes lymphocyte recruitment and retention in both irradiated and abscopal tumors, which drives an increased density of active CD8^{+} T cells in tumors. This increased CD8^{+} T cell activity leads to a significantly increased survival rate over those monotherapy treatment groups.

Two types of immunotherapy that could be combined with RT include checkpoint blockade, such as aCTLA-4 and aPD-1, and immunostimulatory cytokines, such as HD IL-2. Following the rapid increase in the number of patients receiving checkpoint blockade immunotherapies, there were a number of case reports of dramatic responses to combination RT and checkpoint blockade that have

been attributed to the ability of RT to potentiate the response to immunomodulation.[55–58] In general, checkpoint blockade and RT do not have overlapping toxicity profiles, and there is abundant preclinical evidence that RT can be used to potentiate the effectiveness of checkpoint blockade regimens by augmenting antigen presentation, trafficking to the tumor microenvironment, and releasing pro-inflammatory cytokines.[6–8 12 43]

Unfortunately, the dramatic response to a checkpoint blockade and RT combination frequently observed in preclinical models has generally not translated into clinical trials, and the overwhelming majority of clinical data indicate only modest increases in response rates in patients receiving combination RT/checkpoint blockade regimens or no difference in clinical response from patients receiving checkpoint blockade alone.[16 18 59 60] More recently there have been phase II studies demonstrating the potential for increased responsiveness and disease control in metastatic non-small cell lung cancer patients who received stereotactic ablative RT prior to PD-1 blockade.[61 62] However, a clinical trial combining stereotactic RT with HD IL-2 to treat metastatic melanoma and renal cell carcinoma demonstrated a greater than fourfold increase compared with historic response rates for HD IL-2 therapy alone.[17] These early results were developed into a randomized clinical trial comparing HD IL-2 therapy with or without stereotactic RT for the treatment of metastatic melanoma (NCT01416831) that has now finished accrual but has yet to be published. Despite this success, the toxicity of HD IL-2 treatment remains a barrier to a wide adoption of this combination.

NKTR-214 provides an attractive alternative to recombinant HD IL-2 therapy given its ability to potently stimulate T cells and NK cells, its excellent tolerability, long half-life, and ability to deliver therapy in an outpatient setting. This work describes the results of combination NKTR-214 immunotherapy and HD RT for the treatment of fibrosarcoma and colorectal murine tumor models; the experiments were performed using a bilateral tumor model, which enabled us to observe both the direct and abscopal effects of RT. We found synergy between RT and NKTR-214, with combination therapy resulting in statistically significant doubling to tripling of cure rates to 45%–85% of animals depending on tumor type compared with NKTR-214 monotherapy (figure 1). This increase in cure is dependent on CD8$^+$ T cell immunity (figure 1), which we observed to significantly increase in the periphery in animals receiving combination NKTR-214/RT compared with NKTR-214 monotherapy and to correlate with total tumor burden (figure 2).

Phenotypic analysis of these circulating CD8$^+$ T cells revealed a combination therapy-dependent increase in the per cent of CD8$^+$ T cells expressing the costimulatory marker ICOS and the exhaustion marker Tim-3. Notably, circulating Treg cells expressed less PD-1 and ICOS in animals treated with combination therapy compared with NKTR-214 alone (figure 3). We believe that the modulation of these coinhibitory and costimulatory molecules provides a preclinical rationale to evaluate the potential therapeutic synergy of targeting these molecules in conjunction with NKTR-214/RT. Within the tumor microenvironment, NKTR-214/RT combination therapy resulted in increased cytotoxic CD8$^+$ T cell density and increased proliferation, expression of activation/exhaustion markers, and production of both granzyme and effector cytokines compared with monotherapy with NKTR-214 alone (figure 4). Remarkably, these increases were observed in both the treatment side tumor and the abscopal side tumor, which is important in light of common clinical scenarios of metastatic tumor burden where only one or a few individual tumors receive RT. These results, combined with our examination of bulk RNA transcripts from the tumor, suggest HD RT to a single site of disease results in increased trafficking (figure 5) and antitumor activity of tumor-specific CD8$^+$ T cells at distant, unirradiated, sites of disease. However, the mechanism of induction of this expression and the cell type or types mediating recruitment to abscopal sites of disease are not known at this time. Our preliminary experiments suggest either tumor cells or stromal cells as likely candidates, and further exploration of these cells will be the subject of future studies. It is possible that the proliferative burst initiated by combined NKTR-214/RT therapy simply provides additional tumor-specific CD8$^+$ T cells that participate in tumor killing and potentiate further recruitment to unirradiated sites of disease.

Despite tremendous interest in combining modern stereotactic RT with immunotherapy to drive antitumor immune responses, much remains to be elucidated regarding the mechanisms that underlie synergy between these two therapies. Adding RT to a single lesion in the current study resulted in increased CD8$^+$ T cell activity and abundance within the tumor microenvironment compared with treatment with NKTR-214 alone—a response that extended to unirradiated lesions. There is evidence that RT can increase MHC I expression within irradiated tumors,[6] increase the cross-presentation of tumor antigens,[5] trigger a type I interferon response through the stimulator of interferon genes (STING) pathway,[8] and increase expression of cytokines and chemokines required for T cell homing to effector sites.[7 9 43] Interestingly, we observed an increase in expression of the homing markers CCL4, CCL5, and CXCL10 in both irradiated and contralateral unirradiated tumors following combination therapy with NKTR-214/RT, which we did not observe with RT alone or NKTR-214 monotherapy (figure 5). Thus, we believe synergy between the two modalities results from increased homing of functional CD8$^+$ T cell effectors to abscopal sites, which may be the key to the significant increase in systemic tumor clearance and survival observed in our combination treated cohorts.

CONCLUSIONS

This study has significant translational implications for future patients. NKTR-214 immunotherapy has completed a dose escalation clinical trial as monotherapy (NCT02869295) and is now being tested in combination with CTLA-4 and/or PD-1 blockade to treat metastatic melanoma, renal cell carcinoma, non-small cell lung cancer, sarcoma, and triple negative breast cancer (NCT02983045, NCT03282344, NCT03635983).[35] Early results have demonstrated these treatments to be well-tolerated.[33] Stereotactic radiosurgery and hypofractionated palliative RT are standard of care treatments in the majority of patients who will be eligible for future trials with NKTR-214 treatment alone or in combination with PD-1 blockade. While prior preclinical and early clinical work has demonstrated increased response rates in disease treated with combination RT and IL-2 receptor ligation,[17 63 64] to our knowledge NKTR-214 has not been previously combined with RT in a preclinical model, and this demonstrates an exciting new clinical combination that may be immediately relevant in future clinical trial development. We believe that the addition of RT to immunotherapy regimens with NKTR-214 +/− checkpoint blockade may result in dramatically increased response rates within both irradiated and unirradiated sites of disease with minimal increase in toxicity compared with immunotherapy alone.

Author affiliations
[1]Department of Radiation Medicine, Oregon Health & Science University, Portland, Oregon, USA
[2]Department of Cell, Developmental & Cancer Biology, Oregon Health & Science University, Portland, Oregon, USA
[3]Earle A. Chiles Research Institute, Providence Cancer Institute, Portland, Oregon, USA
[4]Nektar Therapeutics, San Francisco, California, USA

ORCID iDs
Joshua M Walker http://orcid.org/0000-0002-0810-4969
William L Redmond http://orcid.org/0000-0002-2572-1731

REFERENCES

1. Begg AC, Stewart FA, Vens C. Strategies to improve radiotherapy with targeted drugs. *Nat Rev Cancer* 2011;11:239–53.
2. Bryant AK, Banegas MP, Martinez ME, *et al*. Trends in radiation therapy among cancer survivors in the United States, 2000-2030. *Cancer Epidemiol Biomarkers Prev* 2017;26:963–70.
3. Solberg TD, Siddon RL, Kavanagh B. Stereotactic body radiation therapy 2012:9–35.
4. Folkert MR, Timmerman RD. Stereotactic ablative body radiosurgery (SABR) or stereotactic body radiation therapy (SBRT). *Adv Drug Deliv Rev* 2017;109:3–14.
5. Reits EA, Hodge JW, Herberts CA, *et al*. Radiation modulates the peptide repertoire, enhances MHC class I expression, and induces successful antitumor immunotherapy. *J Exp Med* 2006;203:1259–71.
6. Sharabi AB, Nirschl CJ, Kochel CM, *et al*. Stereotactic radiation therapy augments antigen-specific PD-1-Mediated antitumor immune responses via cross-presentation of tumor antigen. *Cancer Immunol Res* 2015;3:345–55.
7. Lim JYH, Gerber SA, Murphy SP, *et al*. Type I interferons induced by radiation therapy mediate recruitment and effector function of CD8(+) T cells. *Cancer Immunol Immunother* 2014;63:259–71.
8. Vanpouille-Box C, Alard A, Aryankalayil MJ, *et al*. Dna exonuclease TREX1 regulates radiotherapy-induced tumour immunogenicity. *Nat Commun* 2017;8:ncomms15618.
9. Matsumura S, Wang B, Kawashima N, *et al*. Radiation-Induced CXCL16 release by breast cancer cells attracts effector T cells. *J Immunol* 2008;181:3099–107.
10. Connolly KA, Belt BA, Figueroa NM, *et al*. Increasing the efficacy of radiotherapy by modulating the CCR2/CCR5 chemokine axes. *Oncotarget* 2014;5.
11. Schaue D, Ratikan JA, Iwamoto KS, *et al*. Maximizing tumor immunity with fractionated radiation. *Int J Radiat Oncol Biol Phys* 2012;83:1306–10.
12. Filatenkov A, Baker J, Mueller AMS, *et al*. Ablative tumor radiation can change the tumor immune cell microenvironment to induce durable complete remissions. *Clinical Cancer Research* 2015;21:3727–39.
13. Lee Y, Auh SL, Wang Y, *et al*. Therapeutic effects of ablative radiation on local tumor require CD8+ T cells: changing strategies for cancer treatment. *Blood* 2009;114:589–95.
14. Demaria S, Kawashima N, Yang AM, *et al*. Immune-Mediated inhibition of metastases after treatment with local radiation and CTLA-4 blockade in a mouse model of breast cancer. *Clin Cancer Res* 2005;11:728–34.
15. Dewan MZ, Galloway AE, Kawashima N, *et al*. Fractionated but not single-dose radiotherapy induces an immune-mediated abscopal effect when combined with anti-CTLA-4 antibody. *Clin Cancer Res* 2009;15:5379–88.
16. Formenti SC, Rudqvist N-P, Golden E, *et al*. Radiotherapy induces responses of lung cancer to CTLA-4 blockade. *Nat Med* 2018;24:1845–51.
17. Seung SK, Curti BD, Crittenden M, *et al*. Phase 1 study of stereotactic body radiotherapy and interleukin-2--tumor and immunological responses. *Sci Transl Med* 2012;4:137–74.

18 Twyman-Saint Victor C, Rech AJ, Maity A, *et al*. Radiation and dual checkpoint blockade activate non-redundant immune mechanisms in cancer. *Nature* 2015;520:373–7.

19 Atkins MB, Lotze MT, Dutcher JP, *et al*. High-Dose recombinant interleukin 2 therapy for patients with metastatic melanoma: analysis of 270 patients treated between 1985 and 1993. *JCO* 1999;17:2105.

20 Smith FO, Downey SG, Klapper JA, *et al*. Treatment of metastatic melanoma using interleukin-2 alone or in conjunction with vaccines. *Clin Cancer Res* 2008;14:5610–8.

21 Davar D, Ding F, Saul M, *et al*. High-Dose interleukin-2 (HD IL-2) for advanced melanoma: a single center experience from the University of Pittsburgh cancer Institute. *J Immunother Cancer* 2017;5:74.

22 Fyfe G, Fisher RI, Rosenberg SA, *et al*. Results of treatment of 255 patients with metastatic renal cell carcinoma who received high-dose recombinant interleukin-2 therapy. *J Clin Oncol* 1995;13:688–96.

23 Rosenberg SA. Il-2: the first effective immunotherapy for human cancer. *J Immunol* 2014;192:5451–8.

24 Dutcher JP, Schwartzentruber DJ, Kaufman HL, *et al*. High dose interleukin-2 (Aldesleukin) - expert consensus on best management practices-2014. *J Immunother Cancer* 2014;2:26.

25 Boyman O, Sprent J. The role of interleukin-2 during homeostasis and activation of the immune system. *Nat Rev Immunol* 2012;12:180–90.

26 Krieg C, Létourneau S, Pantaleo G, *et al*. Improved IL-2 immunotherapy by selective stimulation of IL-2 receptors on lymphocytes and endothelial cells. *Proc Natl Acad Sci U S A* 2010;107:11906–11.

27 Létourneau S, van Leeuwen EMM, Krieg C, *et al*. IL-2/anti-IL-2 antibody complexes show strong biological activity by avoiding interaction with IL-2 receptor α subunit CD25. *Proc Natl Acad Sci U S A* 2010;107:2171–6.

28 Jing H, Hettich M, Gaedicke S, *et al*. Combination treatment with hypofractionated radiotherapy plus IL-2/anti-IL-2 complexes and its theranostic evaluation. *J Immunother Cancer* 2019;7:55.

29 van den Heuvel MM, Verheij M, Boshuizen R, *et al*. NHS-IL2 combined with radiotherapy: preclinical rationale and phase Ib trial results in metastatic non-small cell lung cancer following first-line chemotherapy. *J Transl Med* 2015;13:32.

30 Rekers NH, Olivo Pimentel V, Yaromina A, *et al*. The immunocytokine L19-IL2: an interplay between radiotherapy and long-lasting systemic anti-tumour immune responses. *Oncoimmunology* 2018;7:e1414119.

31 Charych D, Khalili S, Dixit V, *et al*. Modeling the receptor pharmacology, pharmacokinetics, and pharmacodynamics of NKTR-214, a kinetically-controlled interleukin-2 (IL2) receptor agonist for cancer immunotherapy. *PLoS One* 2017;12:e0179431.

32 Charych DH, Hoch U, Langowski JL, *et al*. NKTR-214, an engineered cytokine with biased IL2 receptor binding, increased tumor exposure, and marked efficacy in mouse tumor models. *Clin Cancer Res* 2016;22:680–90.

33 Diab A, Hurwitz ME, Cho DC, *et al*. NKTR-214 (CD122-biased agonist) plus nivolumab in patients with advanced solid tumors: preliminary phase 1/2 results of pivot. *JCO* 2018;36:3006.

34 Barroso-Sousa R, Ott PA. Transformation of old concepts for a new era of cancer immunotherapy: cytokine therapy and cancer vaccines as combination partners of PD1/PD-L1 inhibitors. *Curr Oncol Rep* 2018;20:1.

35 Bentebibel S-E, Hurwitz ME, Bernatchez C, *et al*. A First-in-Human Study and Biomarker Analysis of NKTR-214, a Novel IL-2-Receptor Beta/Gamma (βγ)-Biased Cytokine, in Patients With Advanced or Metastatic Solid Tumors. *Cancer Discov* 2019;CD-18-1495.

36 Moran AE, Holzapfel KL, Xing Y, *et al*. T cell receptor signal strength in Treg and iNKT cell development demonstrated by a novel fluorescent reporter mouse. *J Exp Med* 2011;208:1279–89.

37 Newman AM, Liu CL, Green MR, *et al*. Robust enumeration of cell subsets from tissue expression profiles. *Nat Methods* 2015;12:453–7.

38 Huang AY, Gulden PH, Woods AS, *et al*. The immunodominant major histocompatibility complex class I-restricted antigen of a murine colon tumor derives from an endogenous retroviral gene product. *Proc Natl Acad Sci U S A* 1996;93:9730–5.

39 Fan X, Quezada SA, Sepulveda MA, *et al*. Engagement of the ICOS pathway markedly enhances efficacy of CTLA-4 blockade in cancer immunotherapy. *J Exp Med* 2014;211:715–25.

40 Watanabe M, Hara Y, Tanabe K, *et al*. A distinct role for ICOS-mediated co-stimulatory signaling in CD4+ and CD8+ T cell subsets. *Int Immunol* 2005;17:269–78.

41 Fourcade J, Sun Z, Benallaoua M, *et al*. Upregulation of Tim-3 and PD-1 expression is associated with tumor antigen-specific CD8+ T cell dysfunction in melanoma patients. *J Exp Med* 2010;207:2175–86.

42 Avery L, Filderman J, Szymczak-Workman AL, *et al*. Tim-3 co-stimulation promotes short-lived effector T cells, restricts memory precursors, and is dispensable for T cell exhaustion. *Proc Natl Acad Sci U S A* 2018;115:2455–60.

43 Meng Y, Efimova EV, Hamzeh KW, *et al*. Radiation-Inducible immunotherapy for cancer: senescent tumor cells as a cancer vaccine. *Mol Ther* 2012;20:1046–55.

44 Lebbé C, Weber JS, Maio M, *et al*. Survival follow-up and ipilimumab retreatment of patients with advanced melanoma who received ipilimumab in prior phase II studies. *Ann Oncol* 2014;25:2277–84.

45 Hodi FS, O'Day SJ, McDermott DF, *et al*. Improved survival with ipilimumab in patients with metastatic melanoma. *N Engl J Med* 2010;363:711–23.

46 Wolchok JD, Kluger H, Callahan MK, *et al*. Nivolumab plus ipilimumab in advanced melanoma. *N Engl J Med* 2013;369:122–33.

47 Robert C, Thomas L, Bondarenko I, *et al*. Ipilimumab plus dacarbazine for previously untreated metastatic melanoma. *N Engl J Med* 2011;364:2517–26.

48 Ribas A, Puzanov I, Dummer R, *et al*. Pembrolizumab versus investigator-choice chemotherapy for ipilimumab-refractory melanoma (KEYNOTE-002): a randomised, controlled, phase 2 trial. *Lancet Oncol* 2015;16:908–18.

49 Motzer RJ, Escudier B, McDermott DF, *et al*. Nivolumab versus everolimus in advanced renal-cell carcinoma. *N Engl J Med* 2015;373:1803–13.

50 Borghaei H, Paz-Ares L, Horn L, *et al*. Nivolumab versus docetaxel in advanced Nonsquamous non-small-cell lung cancer. *N Engl J Med* 2015;373:1627–39.

51 Reck M, Rodríguez-Abreu D, Robinson AG, *et al*. Pembrolizumab versus chemotherapy for PD-L1-positive non-small-cell lung cancer. *N Engl J Med* 2016;375:1823–33.

52 Gandhi L, Rodríguez-Abreu D, Gadgeel S, *et al*. Pembrolizumab plus chemotherapy in metastatic Non–Small-Cell lung cancer. *New England Journal of Medicine* 2018;378:2078–92.

53 El-Khoueiry AB, Sangro B, Yau T, *et al*. Nivolumab in patients with advanced hepatocellular carcinoma (CheckMate 040): an open-label, non-comparative, phase 1/2 dose escalation and expansion trial. *Lancet* 2017;389:2492–502.

54 Ferris RL, Blumenschein G, Fayette J, *et al*. Nivolumab for recurrent squamous-cell carcinoma of the head and neck. *N Engl J Med* 2016;375:1856–67.

55 Golden EB, Demaria S, Schiff PB, *et al*. An Abscopal response to radiation and ipilimumab in a patient with metastatic non-small cell lung cancer. *Cancer Immunology Research* 2013;1:365–72.

56 Postow MA, Callahan MK, Barker CA, *et al*. Immunologic correlates of the abscopal effect in a patient with melanoma. *N Engl J Med* 2012;366:925–31.

57 Britschgi C, Riesterer O, Burger IA, *et al*. Report of an abscopal effect induced by stereotactic body radiotherapy and nivolumab in a patient with metastatic non-small cell lung cancer. *Radiat Oncol* 2018;13:102.

58 Abuodeh Y, Venkat P, Kim S. Systematic review of case reports on the abscopal effect. *Curr Probl Cancer* 2016;40:25–37.

59 Hiniker SM, Reddy SA, Maecker HT, *et al*. A Prospective Clinical Trial Combining Radiation Therapy With Systemic Immunotherapy in Metastatic Melanoma. *Int J Radiat Oncol Biol Phys* 2016;96:578–88.

60 Maity A, Mick R, Huang AC, *et al*. A phase I trial of pembrolizumab with hypofractionated radiotherapy in patients with metastatic solid tumours. *Br J Cancer* 2018;119:1200–7.

61 Theelen WSME, Peulen HMU, Lalezari F, *et al*. Effect of pembrolizumab after stereotactic body radiotherapy vs pembrolizumab alone on tumor response in patients with advanced Non–Small cell lung cancer. *JAMA Oncol* 2019;5:1276–82.

62 Bauml JM, Mick R, Ciunci C, *et al*. Pembrolizumab after completion of locally ablative therapy for oligometastatic Non–Small cell lung cancer. *JAMA Oncol* 2019;5:1283–90.

63 Yasuda K, Nirei T, Tsuno NH, *et al*. Intratumoral injection of interleukin-2 augments the local and abscopal effects of radiotherapy in murine rectal cancer. *Cancer Sci* 2011;102:1257–63.

64 Younes E, Haas GP, Dezso B, *et al*. Local tumor irradiation augments the response to IL-2 therapy in a murine renal adenocarcinoma. *Cell Immunol* 1995;165:243–51.